

Experimental



2.1 Synthesis

2.1.1 Materials

Chitosan from shrimp shells with $\geq 75\%$ degree of deacetylation was obtained from Sigma Aldrich, USA. Poly (tetramethelene glycol) (PTMG), number-average molecular weight (M_n) 2900g/mol was procured from Sigma Aldrich, USA. 1,6-hexamethulene diisocyanate (HMDI) and Dimethyl formamide (DMF) were taken from Merck, Germany. The catalyst dibutyltin dilaurate (DBTDL) was obtained from Himedia. Mg-Al- PO_4 -layer double hydroxide (LDH) was synthesized via co-precipitation method (Senapati et al., 2016). Organically modified nanoclay, methyl tallow bis-hydroxyethyl quaternary ammonium ion exchanged montmorillonite (Southern Clay; CEC 110 meequiv/100g) (Cloisite 30B) was used as received. Rhodamine B was purchased from Sigma-Aldrich. The antibacterial drug, tetracycline hydrochloride was obtained from Sigma-Aldrich, USA.

2.1.1.2 Synthesis of PU-graft-Chitosan

Polyurethane chain was grafted on to chitosan backbone following two steps as (1) preparation of polyurethane prepolymers, and (2) Copolymerization through grafting. The prepolymer was prepared through condensation reaction between HMDI and PTMG in the $-NCO/-OH$ ratio of 1.05:1 in presence of DBTDL catalyst. The reaction was carried out at 80 °C for 2h in closed vessel. Chitosan was dispersed into glacial acetic acid / DMF mixture in the ratio of 50/50 for overnight to obtain good swollen chitosan and to execute the grafting. The polyurethane prepolymer was cooled down to room temperature and then swollen chitosan was added. The reaction was carried out at 80 °C

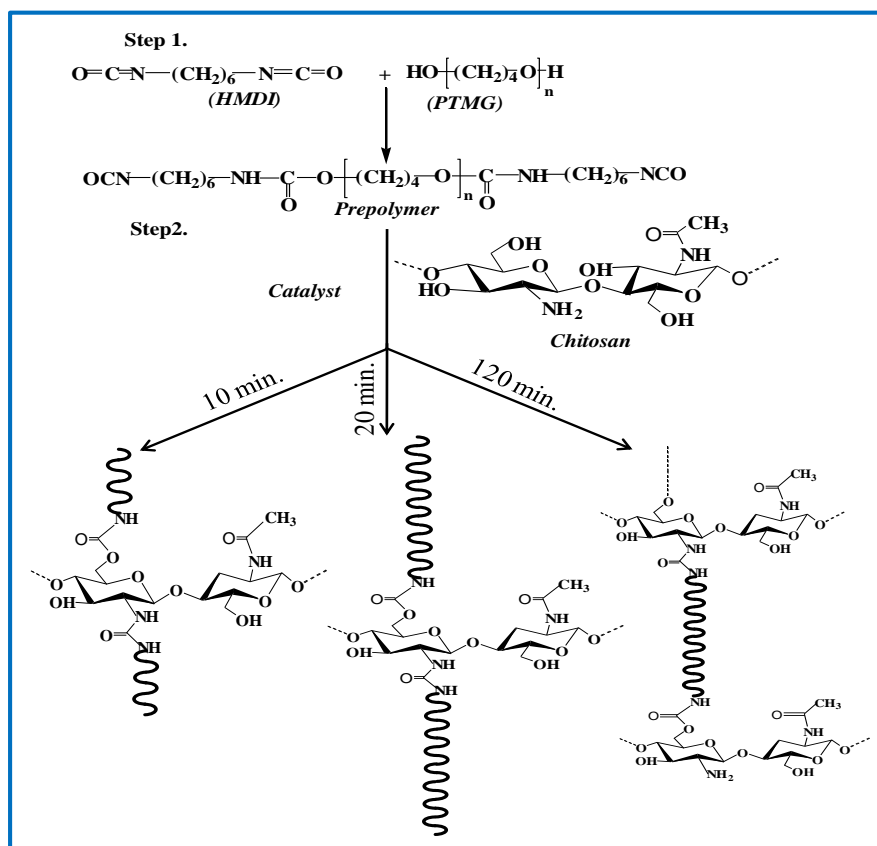


Figure 2.1: Schematic diagram of obtained grafting product of chitosan modified by polyurethane.

under constant stirring for predetermined times mention in **Table 3.1** to prepared PU-graft-CHT with different degree of substitution. After end of the reaction, the reaction mixture was poured into distilled water. Grafted copolymer was isolated through filtration and successively washed with DMF, methanol, acetone to remove the excess pure polyurethane from grafted specimen. The reaction details are shown in **Figure 2.1**.

2.1.1.3 Synthesis of Polyurethane-Chitosan brush

Chitosan was hydrophobically modified through grafting of polyurethane with varying degree of substitution. Grafting was done in two steps as (1) preparation of polyurethane prepolymers with isocyanate end group and (2) copolymerizing it through grafting over

chitosan chain. Polyurethane prepolymer was formed through the reaction between HMDI and PTMG in a –NCO/-OH ratio of 1.05:1 in DMF solvent adding few drops 0.1 wt% DBTDL solution in toluene as catalyst. The reaction was continued for 2 hours at 80 °C to prepare an isocyanate terminated prepolymers in closed reaction vessel. After completion of the reaction, the reaction mixture was cooled down to room temperature and fully swollen chitosan was added to the reaction mixture continuing the reaction for predetermined times (**Table 4.1**) at same reaction condition. After end of the reaction, the reaction mixture was precipitated in distilled water. The grafted product was collected through filtration, and washing with DMF, methanol and acetone successively to remove the unreacted components. The product was completely dried at 60 °C under reduced pressure and copolymers were termed as CHT10 and CHT15 for 10 and 15% grafting on to chitosan as measured through NMR spectroscopy. All the details of the reaction along with the architecture of various copolymers are given in **Figure 2.2**.

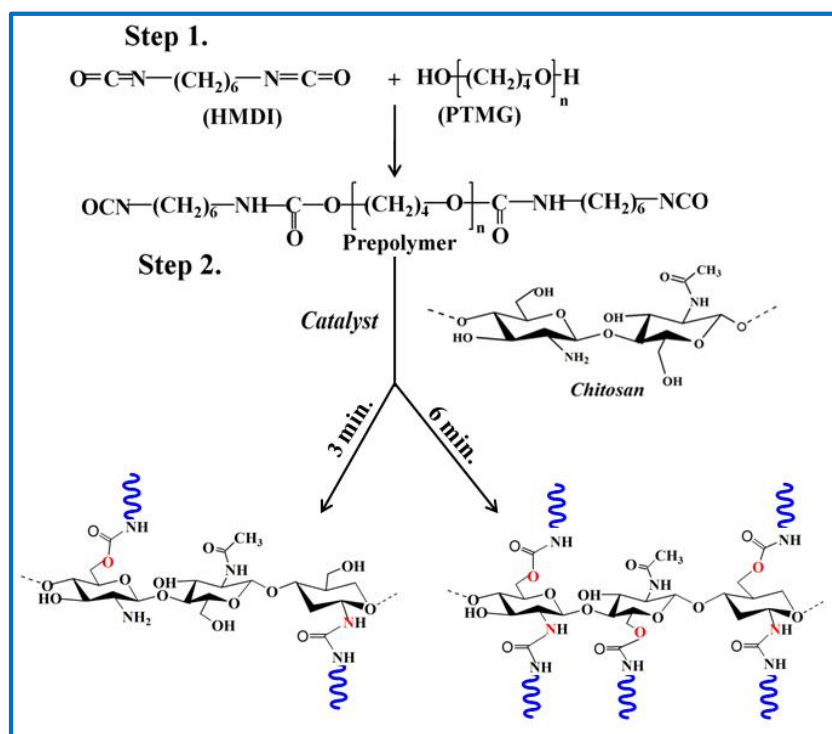


Figure 2.2: Reaction scheme of the polyurethane based chitosan brush copolymers.

2.1.1.4 Preparation of Hydrogel and Scaffold

Hydrogel of Polyurethane graft copolymers were prepared in 0.1 (M) acetic acid medium with a predetermined concentration 1-8% (w/v). In the similar way, Chitosan nanocomposite hydrogel was prepared. The nanoparticles were used like organically modified nanoclay (Cloisite 30B) and Mg-Al-PO₄-layer double hydroxide (LDH).

Hydrogels were pre-cooled at -80 °C for 8 hours and then lyophilized at -80 °C for 36 hours to prepare the scaffolds.

2.2 Characterization

Several characterization techniques were used during the research work. Details of the characterizations process and instrument are given briefly.

2.2.1 Nuclear Magnetic Resonance Spectroscopy (NMR)

NMR spectroscopy depicts the magnetic properties of certain nuclei. It provides detailed information about the structure, dynamics and chemical environment of molecules. The intermolecular magnetic field around an atom in nuclei affects the resonance frequency which gives details of the electronic structure of a molecule and its individual functional groups. Graft copolymers were characterized through ¹³C solid state NMR spectroscopy. Solid-state ¹³C NMR of the samples were performed on a Bruker 400 MHz spectrometer at 100.628 MHz resonance frequency using 4 mm double resonance cross-polarization magic angle spinning probe. Around 100 mg of finely powdered samples were mounted into a 4 mm diameter cylindrical zirconium oxide rotor with a Kel-F end-cap. ¹³C CP/MAS NMR spectrum was recorded with a cross-polarization contact time of 2 ms and a recycle delay of 5s at a MAS speed of 10 kHz. In order to observe the fast relaxing components a 1s recycle delay was used for HP/MAS experiments. Cross-polarization spin-lattice relaxation experiment (CPT1) which is a modified CP inversion recovery

experiment where a single pulse delay was used between carbon pulses instead of a collection of delays was used for the experiments. The single pulse delay should be about five times to that of the lowest relaxing component to observe selectively the most rigid fractions of the polymer. CPT1 experiment was performed with a 5s single pulse delay determined from spin–lattice data of CPXT1 (crosspolarization spin–lattice relaxation experiment, where, X represents heteronuclei). All experiments were carried out with high power proton decoupling during acquisition at an ambient probe temperature (25 °C). All ^{13}C NMR spectra were assigned taking an adamantane as an external reference.

2.2.2 Fourier Transform Infrared Spectroscopy (FTIR)

Fourier transform infrared (FTIR) spectrum was recorded using Nicolet 6700 FTIR. The measurements were carried out at room temperature with a resolution of 4 cm^{-1} taking 64 scan in the range of $400\text{--}4000\text{ cm}^{-1}$. FTIR spectrum mainly focuses on the detection of functional groups and thereby, confirms the chemical modification of molecules.

2.2.3 UV-Visible Spectroscopy (UV-visible)

The UV-visible measurement was performed using JASCO (V-650) spectrophotometer in reflectance mode in the range of 200–800 nm. UV-visible spectra illustrates the electronic transition of the electrons. Different transitions are observed and $n\rightarrow\pi^*$ and $\pi\rightarrow\pi^*$ are of great importance to measure the level of interaction.

2.2.4 X-ray Diffraction (XRD)

X-ray diffraction study was performed using Rigaku miniflex 600 X-ray diffractometer with graphite monochromator using a $\text{Cu K}\alpha$ source having wavelength 0.154 nm. The generator was operated at 40 kV and 20 mA. The samples were placed on quartz sample holder at room temperature and Scanned at the rate of $3^\circ / \text{min}$.

2.2.5 Morphological investigation

The surface morphology of lyophilized hydrogel scaffolds of pure Chitosan and its nanocomposites were investigated through Scanning electron microscope (SEM). The specimens were placed on metal stab with conducting carbon tape and coated with gold using sputtering apparatus before observation. The extent of dispersion of nanofiller in CHT matrix was investigated through Transmission electron microscope (TEM) operating at a voltage of 200 kV.

2.2.6 Thermal Study

Melting behavior and heat of fusion of Polyurethane graft Chitosan copolymers were investigated using differential scanning calorimeter (DSC, Mettler 832) in the temperature range of -25 to 350 °C at the scan rate of 10°/ min. The melting temperature was estimated from the endothermic peak and the heat of fusion was calculated from the corresponding endothermic peak using a computer attached to the instruments. Thermal stability of the chemically modified Chitosan was checked through thermogravimetric analyzer (TGA, Mettler-Toledo) in the temperature range from 40 to 600 °C at the heating rate 20° / min maintaining the inert atmosphere.

2.2.7 Mechanical behavior

Tensile test of the polymer film was carried out using an Instron 3369 at room temperature at an elongation rate of 5°/min. Film was prepared through solvent casting method. Modulus was calculated taking slope of linear region of the Stress-Strain curve and toughness also calculated integrating the area under the Stress – Strain curve. Mechanical response of lyophilized hydrogel scaffold was measured in compression method. The samples were prepared in cylindrical shape. The compression test was carried out up to 70-80% of its original dimension at a cross head speed of 1mm min⁻¹.

Dynamic mechanical properties of the thick film were performed with dynamic mechanical analyzer Q 800 (TA Instruments) in the tension mode. The dynamic responses were measured at constant frequency of 1 Hz with strain amplitude of 15 μm in the temperature range -150 to 200 $^{\circ}\text{C}$ at a heating rate of 3 $^{\circ}$ / min. The samples were prepared in rectangular shape with 25 \times 5 \times 0.22 mm^3 dimension.

Rheological behavior of the hydrogel was studied as a function of frequency and temperature using Rheologica (model: Nova) using parallel plate geometry (25 mm). Frequency sweep measurements were performed at 30 $^{\circ}\text{C}$ with strain amplitude of 0.05 to maintain the linear responses of the sample. The oscillatory shear experiment was performed in the angular frequency (ω) range 0.1 to 600 $\text{rad}\cdot\text{s}^{-1}$. Temperature sweep tests were carried out in the range of 30-90 $^{\circ}\text{C}$ at an oscillation frequency of 1 Hz and the temperature was varied at the rate of 1 $^{\circ}\text{C}$ / min. Steady shear experiment was executed as a function of time (1-400 s) at 30 $^{\circ}\text{C}$ with constant shear rate $\dot{\gamma} = 0.1 \text{ s}^{-1}$.

2.2.8 Contact Angle

Contact angle measurements tell us about the hydrophilic and hydrophobic nature of a material. Contact angle measurements were performed using the Kruss F-100 tensiometer at ambient temperature (25 $^{\circ}\text{C}$). Contact angle was measured in water and three specimen of each sample was tested to obtain good accuracy in result.

2.2.9 Swelling and Deswelling study

The swelling capability of the sample was estimated by gravimetric technique. A known amount of dried sample was immersed in distilled water containing beaker. The sample was taken out from the medium after predetermined time and soaked with tissue paper to remove the excess medium. The swollen specimens were weighed and transferred to the same medium again. The dynamic weight change of dried sample with respect to time was calculated using the equation no. (i)

$$\% \text{ Swelling} = \frac{W_f - W_i}{W_i} \times 100 \dots\dots\dots(i)$$

Where, W_f is the weight of the dried specimen in the swollen state and W_i is the initial weight of the dried specimen. The dried specimens were equilibrated in distilled water for certain period of time and then placed it on 37 °C bath to understand the deswelling kinetics. The weight of the swollen samples was noted with different time intervals and the amount of deswelling is evaluated using the equation no. (ii)

$$\% \text{ of Deswelling} = \frac{W_s - W_t}{W_s} \times 100 \dots\dots\dots(ii)$$

2.2.10 Drug Release assay

In *vitro* drug release study was performed in PBS (pH~7.4) at 37 °C maintaining physiological environment. The antibacterial drug, tetracycline hydrochloride was used as model drug. A standard stock solution of concentration 1 mg /ml was prepared first. The standard curve was drawn taking the absorbance at 358 nm in the concentration range of 1 to 10 mg / ml using UV-visible spectrophotometer (Jasco V-650). The drug embedded specimens were immersed in 100 ml PBS containing beaker and placed in an incubator shaker (50 rpm) at 37 °C. Aliquot from drug containing release medium were collected at constant time interval and same amount of fresh medium was added to the release medium. The absorbance of the collected aliquots was taken at 358 nm and the amount of the drug corresponding to that absorbance was calculated from the standard curve. Encapsulation of the drug in film, hydrogels and scaffolds are 3, 10 and 6 wt%, respectively.

2.2.11 Bio-and Hemocompatibility

2.2.11.1 Platelet preparation

Peripheral venous blood was centrifuged at 200g for 30 min in citrate phosphate dextrose adenine. The platelet rich-plasma (PRP) was incubated with acetylsalicylic acid (1mM) for 15 min at 37 °C followed by the addition of ethylene diamine tetraacetate (EDTA) (5 mM). The platelets were sedimented from the PRP by centrifugation at 600 g for 15 min. Cells were properly washed using buffer A(20 mM HEPES, 138 mM NaCl, 2.9 mM KCl, 1mM MgCl₂, 0.36 mM NaH₂PO₄, 1 mM ethylene glycol tetraacetic acid (EGTA), 5 mM glucose and 0.6 ADPase units of apyrase / ml, pH ~ 6.2 and kept in suspended condition in buffer B (pH ~ 7.4), which was similar to buffer A but without EGTA.

2.2.11.2 Platelet aggregation studies

Platelet aggregation of pure CHT and its graft copolymers were recorded turbidimetrically using an optical lumi-aggregometer (Chrono-log model 700-2). Polymer suspension prepared in PBS was added after incubation of platelet at 37 °C for 1 min under constant stirring (1200 rpm). Platelet aggregation was captured as percent of light transmitted through the samples as a function of time, while the blank represented 100% light transmittance.

2.2.11.3 *Invitro* hemolysis study

Fresh human blood samples were collected from the healthy volunteers. Fresh EDTA was used to stabilize the whole blood samples before experiments. RBCs were separated through centrifugation and purified. Then the RBCs were diluted in 10 ml PBS. To test the hemolytic activity of samples, 1 ml of RBCs suspension ($\sim 0.4 \times 10^8$ cells / ml) was exposed to different concentration of samples in PBS. RBCs suspended in deionized water and PBS represented as positive and negative control, respectively. Samples were

incubated at 37 °C for 4 h in shaking mode followed by centrifugation at 10000 g for 10 min. Absorbance of hemoglobin was taken at 540 nm, with 655 nm as a reference using microplate spectrophotometer (BioTek , model Power Wave XS2, Medispec, India) at 37 °C. Percent of hemolysis was determined using the equation no. (iii)

$$\% \text{ Hemolysis} = \frac{\text{Sample Abs}_{540-655\text{nm}} - \text{Negative control Abs}_{540-655\text{nm}}}{\text{Positive control Abs}_{540-655\text{nm}} - \text{Negative control Abs}_{540-655\text{nm}}} \times 100$$

.....(iii)

2.2.11.4 Platelet adhesion

Platelets were charged onto slides coated with either with BSA (0.1% w/v) or collagen (100 µg/ml) or samples incubated for 30 min at room temperature. After incubation slides were properly washed and fixed with 4% paraformaldehyde to observe the platelet adhesion on immobilized matrix. The adhesion images were captured under fluorescence microscope with phase contrast attachment (Leica model DM LB2, Lab India Instruments).

2.2.11.5 MTT assay

MTT assay gives the information about the cytotoxicity of materials by representing the amount of viable cells. In this process, reduction of tetrazolium component (MTT) into an insoluble dark-purple formazan by the mitochondria of viable cells is determined. Platelets were exposed to different concentrations (2-100 µg/ml) of the materials for 2 h. After that 50 µM MTT was added and incubated for an additional 4 h at 37 °C. Formazan produced by the reduction of MTT was dissolved in 200 µL of DMSO and the absorbance was taken at 570 nm with the help of microplate spectrophotometer at 37 °C. In this study, untreated cells were taken as positive control (100% viable).

2.2.11.6 Measurement of intracellular ROS

The oxidative activity in platelets was measured using reactive oxygen species (ROS) sensitive probe H₂DCF-DA. After diffusion of H₂DCF-DA, the acetate groups in H₂DCF-DA are cleaved by intracellular esterase releasing the corresponding dichlorodihydrofluorescein (DCF) derivative. 20 μM H₂DCF-DA was added to the aliquots of platelet suspension (1×10⁷ cells / ml) and incubated for 20 min at 37 °C in dark followed by the washing of cells with PBS. The ROS generation was expressed in terms of mean fluorescence intensity and analyzed in FL1 channel of flow cytometer (FACSCalibur, BD Biosciences). The platelets were exposed to hydrogen peroxide (H₂O₂) of 10 μM and taken as the positive control.

2.2.11.7 In vitro cell line studies

2.2.11.7.1 Cell culture

NIH 3T3 mouse embryonic fibroblast cells were cultured in Dulbecco's Modified Eagle Medium (DMEM) containing 10% heat inactivated fetal bovine serum, 100 μg/ml streptomycin and 100 U/ml penicillin. The culture was maintained in a humidified CO₂ incubator with 5% CO₂ maintained at 37 °C.

2.2.11.7.2 Cell viability

Cell viability of the hydrogel and scaffold was performed through MTT assay using NIH-3T3 cells. At first, predetermined amount of sterile liquid hydrogel was placed in a 96-well culture plate by using a pipette. Hydrogels were washed with sterile PBS and exposed UV-sterilization. After sterilization culture medium was added to the sample followed by incubation for overnight. After incubation, the medium was removed and washed with PBS. After washing, NIH-3T3 cells were seeded on the surface of the hydrogel at a density of 1×10⁵ cells per well and incubated for 1, 3 and 5 days. The

culture media was replaced with a fresh media after every two days. After end of the reaction, 50 μl of 0.5 mg ml^{-1} MTT solution in DMEM without FBS was added into each well and incubated for 4 hours at 37 $^{\circ}\text{C}$ to produce formazan. Then 100 μl of DMSO was added to each well to solubilize the water-insoluble purple colored formazan. Absorbance was monitored with the help of a Microplate reader (BioTek, USA) at 570 nm and percentage of cell viability was calculated using the equation no. (iv).

$$\% \text{ of cell viability} = \frac{\text{OD of S}}{\text{OD of C}} \times 100 \dots\dots\dots(\text{iv})$$

Where, C is the optical density of control and S is the optical density of test samples.

MTT assay of scaffold was performed in the similar way. First, Scaffolds were cut with 1 mm thickness and placed on the 96-well plate. Sample containing platelets were exposed to UV-sterilization for 4-6 hours and then incubated with the medium for overnight. After incubation, the same procedure was followed as discussed above for the hydrogel.

2.2.11.7.3 Fluorescence studies

Proliferation of cells on hydrogel and scaffold was observed through fluorescence microscopic technique. Cells were seeded on the surface of the hydrogel and scaffold at a density of 1×10^4 cells per well. After desired period, the cells were washed with PBS and stained with acridine orange and incubated for 30 min at 37 $^{\circ}\text{C}$. After incubation, the excess stain was washed with PBS. Images were captured using fluorescence microscope, Leica.

2.2.12 Antibacterial activity study

The antibacterial activity of antibacterial drug loaded hydrogel was checked on gram negative bacteria *E. coli* through zone of inhibition experiment. First, the bacteria were cultured in nutrient agar medium. Bacteria were spread on surface of the plate uniformly via sterile spatula. Drug loaded hydrogel samples were gently placed over the solidified

agar gel after complete proliferation of bacteria and incubated at 37 °C for 24 h to check the zone of inhibition.

2.2.13 Animal Study

2.2.13.1 Animal

In vivo biodistribution study and in vivo gelation study was carried out with Six Sprague-Dawley rats (6-8 weeks, ~ 300g). All the animals were provided a standard laboratory with proper diet and water after and before the experiments. The experiments were carried out with the recommendation by the animal ethics committee of Banaras Hindu University (Letter No: Dean/2016/CAEC/193).

2.2.13.2 Absorption and tissue distribution study of CHT and PU-graft-CHT (CHT20)

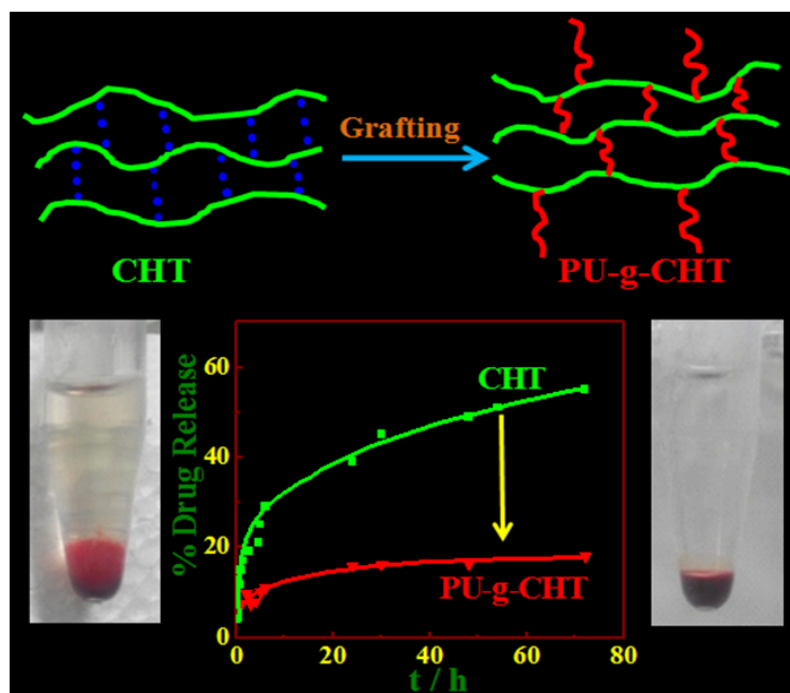
First, Chitosan and (CHT20) were dissolved in 0.1 (M) acetic acid. RhoB was dissolved in water and added to those polymer solutions. The mixture was stirred for overnight at room temperature in dark room. After end of the reaction, RhoB labelled CHT and CHT20 were obtained through the precipitation of the reaction mixture in excess acetone followed by drying through lyophilization. Biodistribution of the materials was carried out through the oral administration of fluorescent tagged materials to the 12h fasted mice (body weight 20-24 mg). RhoB labelled samples were prepared in PBS (pH~7.4) at concentration of 10g/l. Then 0.5 ml (at the dose of 500mg/kg) of the stock solution was administered. The mice were sacrificed at predetermined time to measure the absorbed amount of materials taking blood, liver, kidney, heart, spleen, thymus and lungs. The collected blood samples were suspended in 3 ml of 0.5(M) HCl for overnight at room temperature. Organs were homogenized by glass homogenizer followed by addition of 3 ml of 0.5(M) HCl. Insoluble parts were separated through centrifugation at 3000rpm for 30 min. Then 0.50 ml of solution of the sample was mixed with 3.50 ml phosphate buffer

solution (PBS, pH ~7.4). Fluorescence intensity of the samples was measured by using Fluorescence plate reader. The emission (EM) wavelength was 627 nm and excitation (EX) wavelength was 553nm during the measurements. The obtained fluorescence intensities were by the administrated corresponding Rhodamine-B tagged material. Three mice were sacrificed at a constant time after a administration of one dose of each sample and the data given were the mean \pm SD (n=3). The kidney, liver and spleen were taken out from mice after 4 h administration of PBS (saline) and RhoB-CHT20 for histopathological examination. Then the organs were fixed with 10% formalin and embedded into paraffin. Organs were stained with hematoxylin – eosin (HE) before observation by light microscopy. The animal studies were performed with the permission of Laboratory Animals Division, Central Drug Research Institute (Lucknow, India), and the Laboratory Animal Welfare Committee of the Institute of Medical Sciences, Banaras Hindu University.

2.2.13.3 *In vivo* gelation study

The graft copolymer CHT15 is chosen to understand the *in vivo* gelation study. Six Sprague-Dawley rats (6-8 weeks, ~ 250 g) were used for the experiment with the recommendations of Laboratory Animals Division, Central Drug Research Institute (Lucknow, India) and the Laboratory Animal Welfare Committee of the Institute of Medical Sciences, Banaras Hindu University. The graft copolymer (1 ml) with the concentration of 6% (w/v) was subcutaneously injected on the right dorsal side.

Polyurethane-grafted-chitosan for controlled drug delivery



3.1 Introduction

In the last few decades, great attention has been paid to the Chitosan technology for the biomedical application. Chitosan is one of the most exciting biopolymers, composed of β -(1,4) linked 2-deoxy-2-amino-D-glucopyranose and partially of β -(1,4) linked 2-deoxy-2-acetamido-D-glucopyranose [Onishi et al. 1999; Kumar et al., 2004]. Chitosan is obtained by alkaline deacetylation of chitin which is the major component of the exoskeletal in crustaceans. Various biomaterials of chitosan and its derivatives have been developed for its use in pharmaceuticals applications because of its nontoxic, biodegradable and biocompatible nature [Muzzarelli et al., 2005; Rinaudo et al., 2006; Ifuku et al., 2010; Xiuqing et al., 2009; Hsieha et al., 2006; Yamamoto et al., 1997; Risbud et al., 2000]. Chitosan is extensively used in different field such as membrane, drug delivery system, gene delivery, cell culture, tissue engineering, biosensors, and scaffold generation [Smitha et al. 2006; Lubben et al., 2001; Berthold et al., 1996; Agnihotri et al., 2004; Trindade et al., 2001; Jiang et al., 2006; Chen et al., 2005; Mao et al., 2003; Lin et al., 2005; Wang et al., 2003; Gingras et al., 2003; Du et al., 2007]. Chitosan is insoluble in most common organic solvents and water which limit its application in various fields. Therefore, chitosan have been chemically modified for their possible use in controlled release and targeted delivery of pharmaceuticals [Oliveiraa et al., 2006; Kumar et al., 2000; Bodnar et al., 2005]. Some of these materials are self assembled and have the capability to form nanoparticles for controlled release and targeted delivery of bioactive molecules. Chitosan derivatives like N-alkyl-O-sulfate, crosslinked chitosan and O-carboxymethylate, as well as derivatives containing hydrophobic branches on chitosan backbone have tremendous potential in biomedical applications [Bodnar et al., 2005; Zhang et al., 2003; Zhang et al., 2004]. N-alkyl-O-sulfatenanomicelles shows slow release behavior of hydrophobic anticancer drug,

paclitaxel [Prabaharan et al., 2005]. Mucoadhesive and penetration properties can also be enhanced through chemical modification of chitosan [Brar et al., 2003]. Chitosan derivatives are extensively used in biomedical application which increase the use of crab and shrimp shells and similarly, enhance the growth of seafood industry. Now a day, synthesis of blood compatible polymeric biomaterials have been drawing great attention. In current situation, designing of biomaterials based on natural materials are of great attention. Highly hydrophilic nature and its fast drug release pattern make pure chitosan not suitable for sustained drug delivery and tissue engineering purpose. Further, poor mechanical properties of chitosan limit its application as suitable biometrics [Xu et al., 2008; Lin et al. 2005]. Various properties are such as excellent mechanical property, good thermal stability, increasing anticoagulant, low hydrophilicity, and so on should be improved.

In this chapter, Chitosan is chemically modified for the improvement of the various properties. Chemical modification of chitosan is done through the grafting of isocyanate terminated polyurethane (prepolymer) on to chitosan molecules with various degree of substitutions to control the hydrophilic nature. Network structure has also been obtained through the crosslinking of chitosan molecules with polyurethane bridges. Grafting is confirmed through the different spectroscopic techniques like Solid state ^{13}C NMR, FTIR, UV-visible. Solubility, swelling profile and contact angle measurement clearly indicates the hydrophobic modification followed by crosslinked structure. Thermal and mechanical properties; especially the relaxation behavior has been performed to understand the effect of grafting. The network structure structure on drug release has been revealed to develop a sustained release system. The biocompatibility including hemo compatibility of this new class of material has been checked through MTT assay, platelet adhesion, hemolysis, and reactive oxygen species generation and found suitable for tissue

engineering and drug delivery. Hence, novel drug delivery systems have been designed to control the release kinetics to regulate distribution and to minimize the toxic side effects so as to enhance the therapeutic efficiency of a given drug.

3.2 Results and discussions

3.2.1 Evidence of grafting

Polyurethane chain extension on chitosan backbone has been carried out through the reaction between isocyanate terminated polyurethane pre polymer and hydroxyl/amine group containing chitosan. Solid state ^{13}C NMR has been used to confirm the grafting and calculate the degree of substitution. **Figure 3.1a** represents the ^{13}C NMR spectrum of pure CHT, pure prepolymer and their graft copolymers. Each peaks of CHT and PU are assigned on the basis of literature reports [Ishida et al., 1996; Saito et al., 1987; Kavianiinia et al., 2012]. The grafting of polyurethane onto chitosan is occurred through the formation of urea (-NHCONH-) or urethane linkage (-OCONH-), with either reaction between $-\text{NH}_2$ at C_2 position or $-\text{OH}$ at C_6 position of the chitosan with the prepolymer PU. ^{13}C NMR spectrum shows that chitosan peaks are remain unchanged; instead of two new peaks at 26.9 and 71 ppm corresponding to the PU are observed in the copolymers.

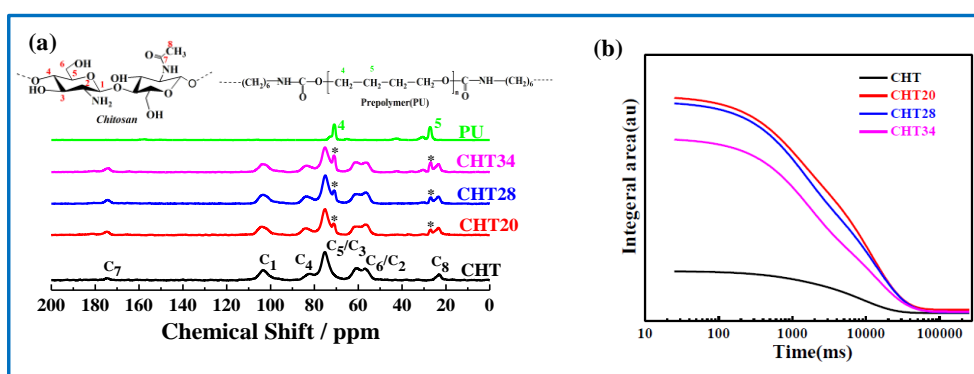


Figure 3.1: (a) ^{13}C solid state NMR Spectra of chitosan, PU and their graft copolymers as indicated; (b) Graphical representation of Spin Lattice Relaxation Time (T_1).

It is interesting to note that these peaks intensity is gradually increased with increase of time of reaction as consequence of greater incorporation of PU chain in CHT backbone at longer reaction time. The degree of substitution has been calculated from the NMR peak area of the deconvulated peak. The copolymers are termed as CHT20, CHT28 and CHT34, where digit after CHT represents the percentage of degree of substitution (**Table 3.1**). The degree of substitution per chitosan monomeric unit has been calculated from the equation no. (v).

$$\text{DS \%} = \frac{\text{Area of } I_{26.9\text{ppm}}}{\text{Area of } I_{26.9\text{ppm}} + \text{Area of } I_{23.35\text{ppm}}} \times 100 \dots\dots\dots (v)$$

Table 3.1: Reaction conditions and nomenclatures of the graft copolymers.

Sample Identification	Degree of substitution	time of reaction	
		Step 1 (h)	Step 2 (min.)
CHT 20	20	2	10
CHT 28	28	2	20
CHT 34	34	2	120

Table 3.2: ^{13}C Spin lattice relaxation time (T_1 , s) for chitosan and its graft copolymers for indicated carbon positions.

CHT	CHT 20	CHT 28	CHT 34
10.1 (C_2), 0.84 (C_6)	11.8 (C_2), 0.92 (C_6)	13.4 (C_2), 1.1 (C_6)	13.6 (C_2), 1.4 (C_6)

This is worthy to mention that DS increases with increase reaction time as newer sites are grafted and longer chain are attached with the CHT chain leading to crosslinking between CHT molecules through PU chains. There are different positions in the chitosan molecule

from which PU chain extension can initiate, therefore it is very important to locate the actual reaction sites. To understand the dynamics of various carbon atoms of CHT Spin-lattice relaxation time (T_1) has been measured [Breitmaier et al., 1975]. It is observed that relaxation time of C_2 and C_6 nuclei are considerably affected with degree of substitution (**Table 3.2**). Systematic increase of T_1 with DS both for C_2 and C_6 nuclei indicating slower dynamics arising from longer PU chains attached. Relaxation behavior as a function of time has shown in **Figure 3.1b** exhibiting a relaxation peak at higher time. Therefore, it is clear from spin – lattice relaxation time (T_1) that rigidity occurs in C_2 and C_6 nuclei with increase in reaction time as compared to other site suggesting chain extension at those sites. The chain extension from the specific carbon atom has been shown in **Figure 3.2**.

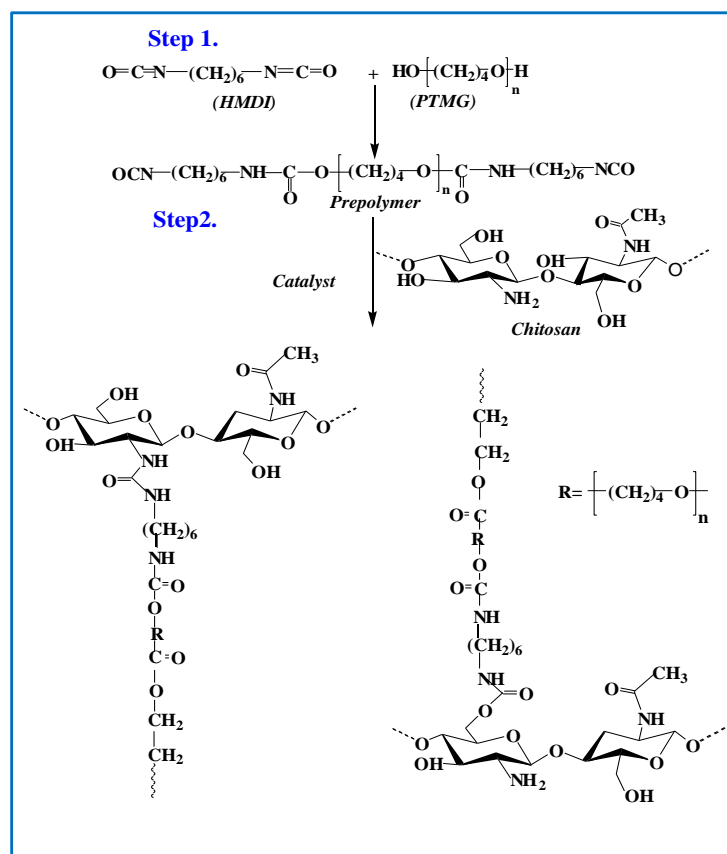


Figure 3.2: Schematic diagram of obtained grafting product of chitosan modified by polyurethane.

Polyurethane grafting on chitosan has been also characterized from FTIR spectroscopic technique. FTIR spectra of pristine CHT and its copolymers are shown in **Figure 3.3a**. The well known characteristics peaks (**Figure 3.3b**) of chitosan are observed at 1650 and 1580 cm^{-1} for N-H and O-H stretching vibration of inter- and intra-molecular hydrogen bonds appears from the $-\text{NH}_2$ and $-\text{OH}$ groups of the chitosan molecule [Chen et al., 2013; Kolhe et al., 2003]. The broad band of pure CHT at 3370 cm^{-1} becomes narrower

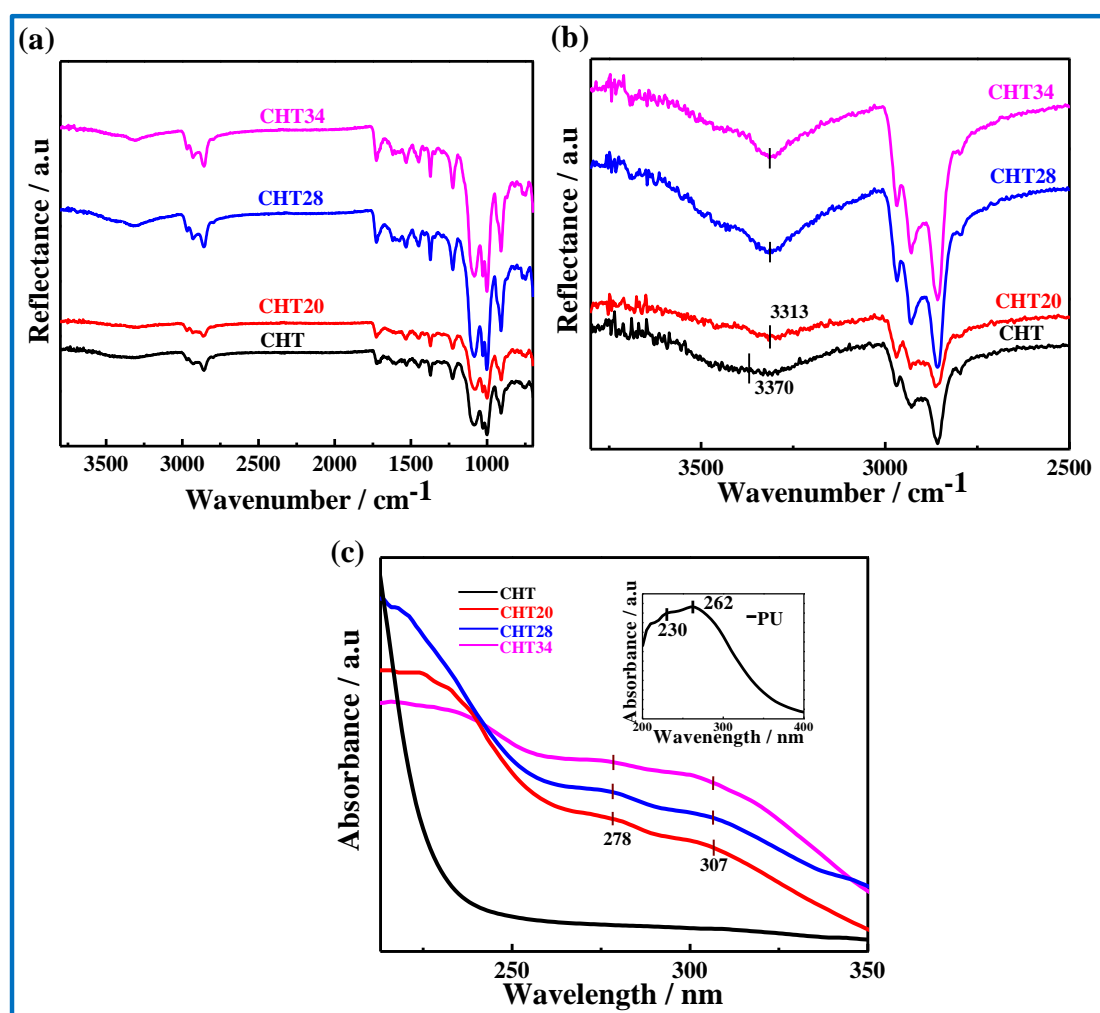


Figure 3.3: (a) FTIR Spectra of CHT and modified CHT with different DS; (b) FTIR Spectra of CHT and its indicated copolymers. The vertical lines indicate the peak positions; (c) UV- Visible spectra of CHT and its indicated copolymers. The vertical lines indicate the peak positions. Inset figure represent the UV-Vis pattern of pure PU showing absorption peaks.

as well as shifted to the lower region at 3313 cm^{-1} in graft copolymers with increasing the degree of substitution suggesting the inter- and intra-molecular hydrogen bonding become weak as the $-\text{NH}_2$ and $-\text{OH}$ groups of CHT have been transformed into corresponding urea and urethane linkages through the reaction between CHT and PU. The shifting of the band is mainly due to the interaction between grafted PU and CHT molecules mainly due to dipolar interaction including hydrogen bonding. The UV-Vis spectra of pure chitosan, prepolymer polyurethane, and its graft copolymers are shown in **Figure 3.3c**. There is no absorption peak for the CHT in the range of 200-400 nm while PU shows one band at 230 and 318 nm due to the $\pi - \pi^*$ and $n - \pi^*$ transition, respectively [Chen et al., 2005]. These results are in good agreement with the literature reported value of grafted chitosan [Liu et al., 2014; Bozic et al., 2012].

3.2.2. Effect of grafting on hydrophilicity

CHT is soluble only in dilute mineral acid while PU is soluble in DMF. The solubility of the copolymers has been checked in 0.1 M acetic acid and in acetic acid / DMF mixture in the ratio of 70/30. The grafted copolymer CHT20 is soluble in both acetic acid and acetic acid/DMF mixture, whereas CHT28 is partially soluble in 0.1 M acetic acid but soluble in acetic acid/DMF mixture but CHT34 is insoluble in both the solvents. It is evident from the solubility tests that slightly longer grafting of PU chain makes CHT partially soluble in acetic acid solution while crosslinking of CHT at longer reaction time (CHT34) convert them into insoluble system. Swelling studies provide important information of the extent of crosslinking in a polymer network [Flory et al., 1953]. The swelling behavior of pure CHT and its graft copolymers are shown in **Figure 3.4a**. Graft copolymers with higher DS exhibit poor swelling. The swelling ability of the copolymers decreases considerably with increase in crosslink density. Swelling behavior of pure CHT has been

presented in the inset of **Figure 3.4a** showing very high swelling (6000%) of pure CHT due to its high hydrophilic nature and it can be tuned up to 200% by controlling the DS or crosslink density through grafting. Grafting of polyurethane on chitosan transform the polymer toward hydrophobic nature as evident from the higher contact angle of copolymers as compared to pure CHT (**Figure 3.4b**).

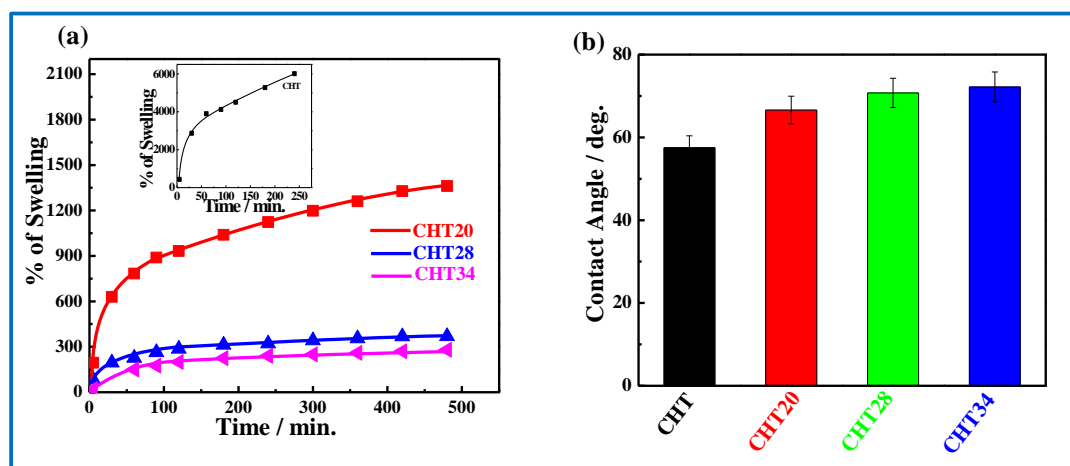


Figure 3.4: (a) Swelling profile of chitosan (inset figure) and its indicated graft copolymers in acetic acid and DMF mixture; (b) Contact Angle of CHT and its copolymers.

Further, the enhancement of the contact angle of the copolymers with increasing DS indicates wrapping up hydrophobic PU on CHT molecules. However, the degree of swelling systematically decreases to 1360, 370 and 280% for CHT20, CHT28 and CHT34, respectively, which is nicely correlated with the increase in contact angle as 66.6, 70.7 and 72.2° for the same order of specimen. However, the solubility, swelling ability and contact angle of grafted and crosslinked chitosan play an important role as a drug carrier.

3.2.3 Effect of grafting in thermal and mechanical properties

Thermal properties of pure chitosan and its graft copolymers are analyzed using TGA and DSC thermograms. **Figure 3.5a** shows the mass loss curves, evaluated under nitrogen atmosphere for pristine CHT, PU and graft copolymers. Pure Chitosan shows one step degradation while graft copolymers show two step of degradation. The initial mass loss observed in the temperature range 45-150°C which is associated with the loss of adsorbed water molecules due to hydrophilic nature of pure Chitosan. The second step degradation starts at 281°C with 50% weight loss which is related to the decomposition of chitosan [Kyzas et al., 2014; Ganguly et al., 2011]. The third step weight loss in graft copolymers corresponds to the PU degradation which occurs at ~400°C. The thermogravimetric analysis is used to find out the thermal stability of chitosan where it is expected to decrease its weight with increasing degree of substitution due to disappearance of hydrogen bonding associated with N-acetyl and free amino groups in graft copolymers [Welsh et al., 2002]. Pure prepolymer (PU) shows single stage degradation at higher temperature (395°C) as compared to the pure Chitosan and completes at 450 °C. On the other hand, CHT shows 60% degradation due to the formation of carbon shoot which is gradually enhanced for the graft copolymers.

DSC thermograms of chitosan, prepolymer (PU) and graft copolymers are shown in **Figure 3.5b**. Chitosan shows a broad endothermic peak at 50 °C which is attributed to the loss of absorbed water and another exothermic peak at 307 °C is due to the decomposition of chitosan which is in good agreement with the TGA analysis [Wan et al., 2006; Rinki et al., 2009].

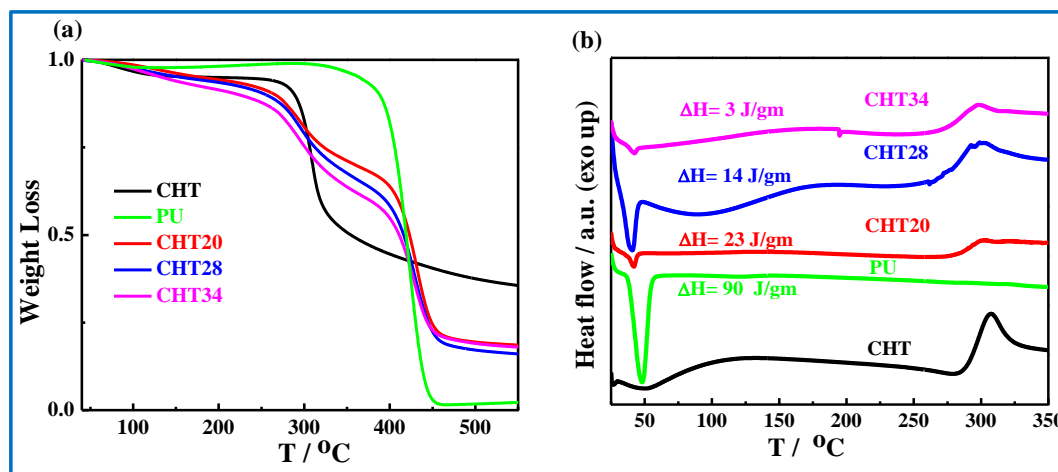


Figure 3.5: (a) TGA and (b) DSC thermograms of CHT and its graft copolymers. The heat of fusion gradually decreases with increasing DS as mentioned.

Prepolymer (PU) shows a sharp endotherm at 48.1 °C indicating its melting point while the graft copolymers show melting peak at ~ 40 °C. The lowering of melting temperature is presumably due to the dilution effect and greater interaction between grafted PU chains and CHT chains. The interactions are further well reflected in reduced heat of fusion (ΔH) of copolymers as compared to pure PU. ΔH gradually decrease with increasing degree of substitution due to the reduction in crystalline part after crosslinking [Ganguly et al., 2011]. However, chitosan does not exhibit any characteristic glass transition temperature (T_g) in its DSC curve. It is very well known that chitosan is a semicrystalline polymer and shows strong intra- and inter-molecular hydrogen bonding along with a rigid amorphous phase of its heterocyclic units. The variation in heat capacity corresponding to the change in specific volume near T_g is too small to be detected by using DSC. A more sensitive technique (DMA measurement) has been used to detect the T_g . Dynamic mechanical analysis (DMA) is a sensitive tool to investigate the relaxation process associated with the molecular motion in a polymer [Riga et al., 2003]. The dynamic mechanical behavior of CHT and its graft copolymers in the temperature range of -150 to

200 °C measured at a frequency of 1 Hz has shown in **Figure 3.6**. Pristine CHT film shows two types of relaxations at -20 °C, β relaxation characteristic of the local motion of side chain groups in chitosan molecule and another at 118 °C, α relaxation or glass transition temperature (T_g). Mucha et al. reports that the β relaxation as typical water relaxation, and the decrease of this temperature for graft copolymer (-30 °C) is attributed to disappearance of hydrogen bond arising from the grafting reaction in -OH or -NH₂ linkages of CHT [Mucha et al., 2005]. The glass transition (T_g) temperature for the graft copolymers decreases to 104 and 102 °C for CHT20 and CHT28, respectively. Intra- and intra-molecular hydrogen bonding in chitosan matrix become weaker as the amount of free -NH₂ and -OH groups decreases with the increase in degree of substitution which is mainly responsible for the decrease decrease in glass transition temperature of the graft copolymers. The various literature reports that the chitosan shows different T_g ranging from -23 to 203 °C [Wan et al., 2006; Garrido et al., 2006; Garrido et al., 2007]. The storage modulus (E') is also decreased with increasing the degree of substitution in graft copolymer and exhibit the values of 10.4, 4.6 and 3.2 GPa for CHT, CHT20 and CHT28, respectively, for similar reason. It is important to note that the measurement of CHT34 is not possible because of its brittle nature arising from highly crosslinked behavior. Loss modulus (E'') of the graft copolymers substantially decreases as compared to pure CHT due to increased rigidity resulting from the grafting of PU chains onto CHT backbone. Stress-strain curves of CHT and its copolymers under uniaxial tension have shown in **Figure 3.7a**. Young's modulus decreases for graft copolymers in comparison to the pure CHT (**Figure 3.7b**) as observe in DMA measurements.

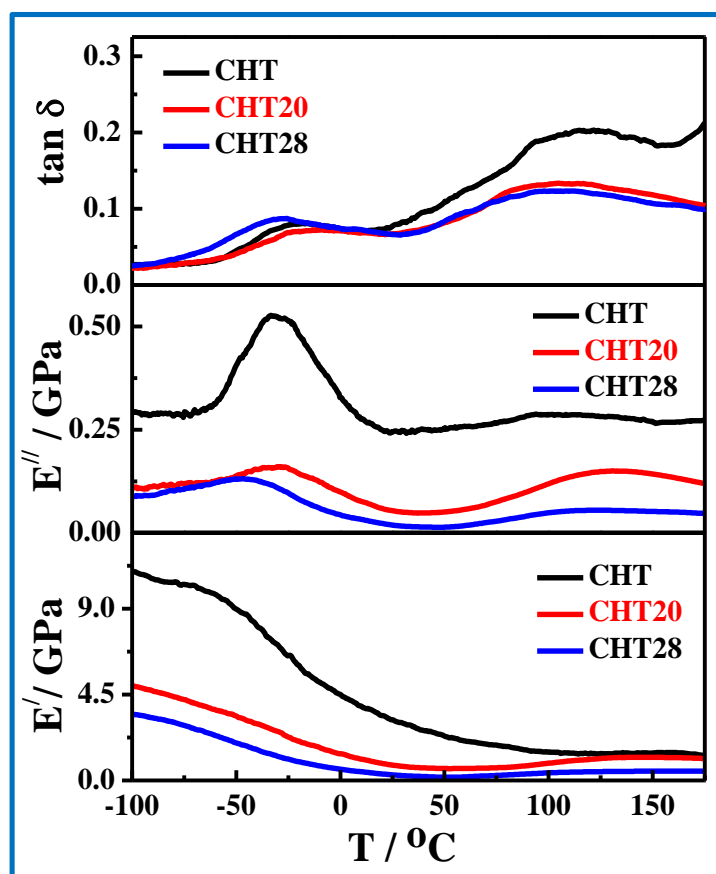


Figure 3.6: Dynamic mechanical responses of pure CHT and its graft copolymers as a function of temperature in tensile mode, $\tan \delta$ curves (top), loss modulus (middle) and storage modulus (bottom).

Chitosan shows high modulus because of its extensive hydrogen bonding. On contrary, grafting in $-\text{OH}$ and $-\text{NH}_2$ groups possibility of forming hydrogen bond is drastically reduced causing a flexible system in the graft copolymers. The percentage elongation at break substantially increases in graft copolymers with a general trend of decreasing elongation at break for greater degree of substitution. Moreover, the toughness increases for graft copolymer as compared to the pristine CHT, except for CHT34 which is a highly crosslinked system (**Figure 3.7c**). Thus, both steady state and dynamic measurements of mechanical properties clearly demonstrate that the flexibility nature of CHT molecules enhances along with the three dimensional network structure in graft copolymer with increasing the degree of substitution. Therefore, graft copolymers have

strong potential for its use as controlled drug delivery system with their added flexibility and network structure.

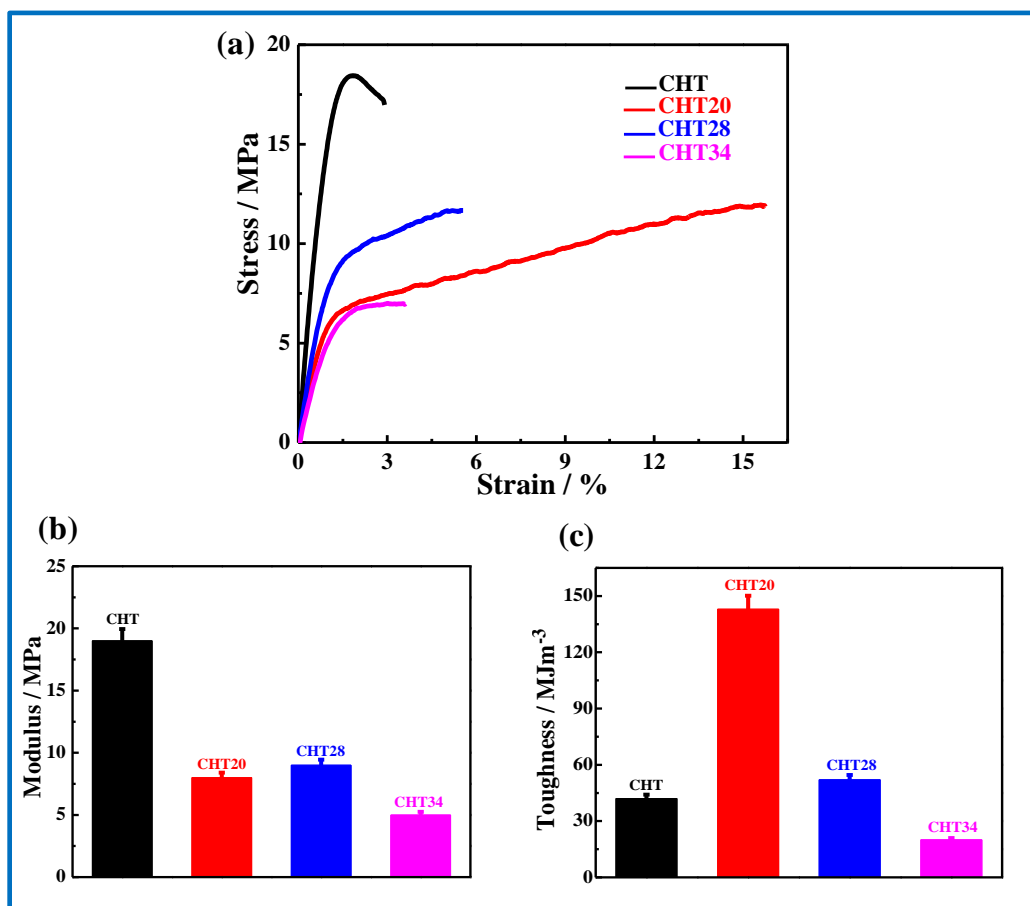


Figure 3.7: (a) Stress – Strain curves for pure CHT and its graft copolymers; (b) modulus and (c) toughness of CHT and its indicated copolymers.

3.2.4 Controlled drug delivery

The controlled drug delivery systems supply a biological molecule depending on the need of the physiological environment over a required time period maintaining the drug level in the body within the therapeutic window. *In vitro* drug release kinetics are performed in phosphate buffer solution (pH~ 7.4) at 37 °C using antibacterial drug, tetracycline hydrochloride loaded biocompatible and hemocompatible pure CHT and polyurethane grafted Chitosan films. The cumulative percentage release of tetracycline hydrochloride as a function of immersion time has shown in **Figure 3.8a**. The sustained release of drug

from PU grafted CHT copolymers is observed as compared to pure CHT. Pure CHT shows fast drug release kinetics and remains as such for longer period of time and 60% of total drug is released in 72 hrs. On the other hand, gradually sustained release has been observed in chemically modified Chitosan with higher degree of substitution (only 15% release for CHT34 in 72 hrs). Moreover, the burst release behavior completely disappears in graft copolymers and the observed cumulative releases are 60, 30, 20 and 15% for pure CHT, CHT20, CHT28 and CHT34, respectively at 72 hrs. Although, the graft copolymers show low value of absolute drug release but the value gradually increase with time as evident in case of CHT34. A comparative study shows that 18% of drug release in 0.8, 2, 18 and 72 hrs in pristine CHT, CHT20, CHT28 and CHT34, respectively suggesting sustained release behavior in graft copolymers as compared to pure Chitosan. Drug release from the polymer matrix mainly depends on the couple of steps like liquid penetration into the matrix, dissolution of the drug and diffusion of drug out of the matrix are the three distinct steps [Deban et al., 2009]. Any of these process may be the rate determining steps for drug release phenomena. It is observed that the diffusion of the drug molecules from the graft copolymers is significantly delayed as compared to the pure CHT. Graft copolymers exert greater extent of network structure because of crosslinking with increase in degree of substitution on chitosan backbone. Denser network is produced with increase in crosslinking. A denser network restricts swelling behavior and simultaneously prevents the diffusion of the drug molecules from the network structures to the release medium. *In vitro* drug release kinetics from the graft copolymers are best fitted with the Korsmeyer-Peppas model. The obtained exponent ' n ' values are 0.27, 0.11, 0.13 and 0.21 for CHT, CHT20, CHT28 and CHT34, respectively, indicating the Fickian ($n < 0.45$) nature of drug diffusion from CHT and its graft

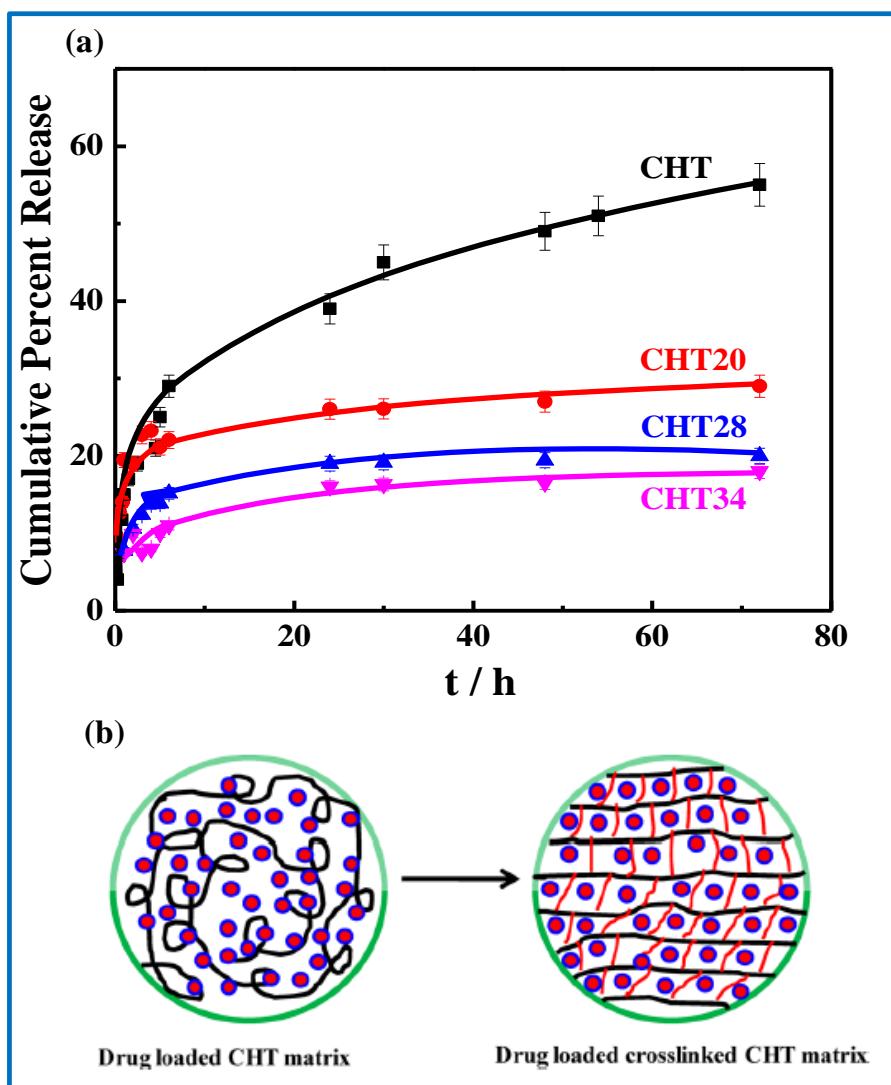


Figure 3.8: (a) Cumulative drug release profile for CHT and its indicated graft copolymers. The solid lines are the guide to the eye; (b) Drug release from pure polymer and its grafted copolymer showing faster in pure CHT against sustained release from network structure in graft copolymer.

copolymers (**Figure 3.9 and Table 3.3**). However, Zero order, firstorder and Higuchi models are also checked but the obtained correlation coefficient (r^2) values corresponding to those models are not satisfactory where is Korsmeyer-Peppas model is a perfect fit. Hence, the slow diffusion of the drug is strongly influenced by the poor swelling ability of the graft copolymers as compared to the pure CHT. A schematic model has been proposed in **Figure 3.8b** to understand the controlled release of the drug from pure polymer and graft copolymers. Extra covalent bonds arising from the grafting of PU on to

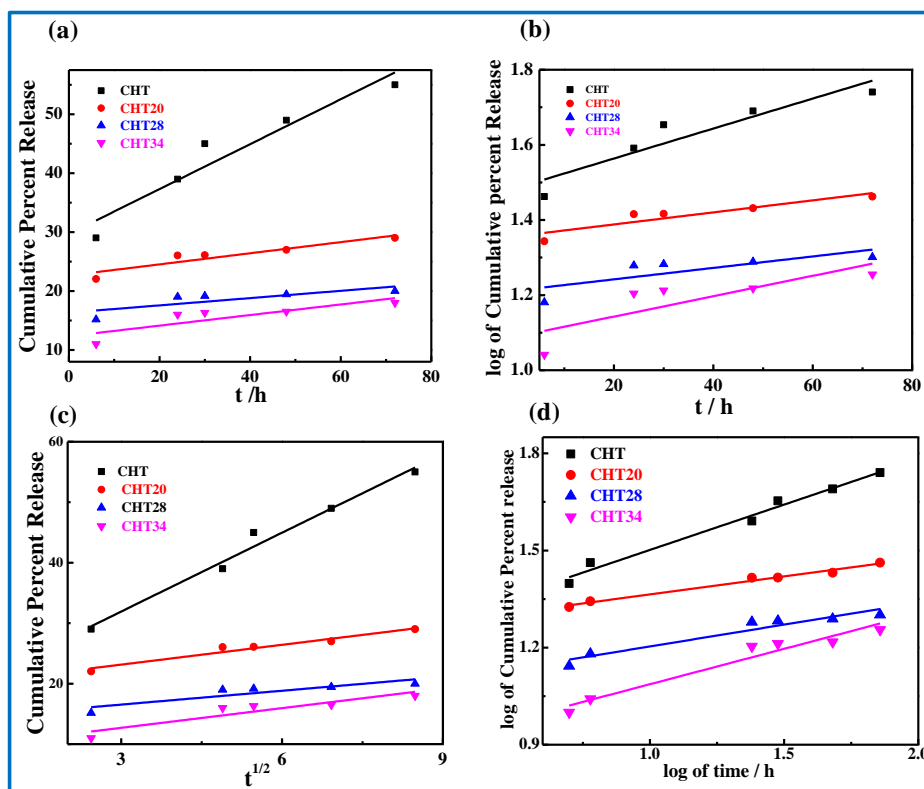


Figure 3.9: Different mathematical model for drug release mechanism (a) Zero order model, (b) First order model, (c) Higuchi model, (d) Korsmeyer- Peppas model.

Table 3.3: Release rate constant (k), correlation coefficient (r^2) and diffusion release exponent (n) obtained using different mathematical models for drug loaded CHT and their respective copolymers.

Sample	Zero Order		First Order		Higuchi		Korsmeyer-Peppas	
	K	r^2	K	r^2	K	r^2	n	r^2
CHT	0.38 ± 0.062	0.90	0.0039 ± 0.008	0.83	4.34 ± 0.3	0.97	0.27 ± 0.01	0.97
CHT20	0.09 ± 0.020	0.83	0.0016 ± 0.003	0.79	1.09 ± 0.1	0.93	0.11 ± 0.006	0.98
CHT28	0.061 ± 0.026	0.52	0.0015 ± 0.0006	0.49	0.76 ± 0.2	0.73	0.13 ± 0.01	0.90
CHT34	0.08 ± 0.032	0.62	0.0027 ± 0.001	0.55	1.08 ± 0.2	0.26	0.21 ± 0.02	0.93

the Chitosan backbone creates the network structure and slow down the diffusion of the drug molecules from the cage like structure of the graft copolymers. In short, drug release kinetics can be controlled by suitable choice of graft copolymer.

3.2.5 Chemically modified Chitosan as biomaterial

Materials injected intravenously for biomedical applications, like implant, biosensor, drug delivery and cell imaging before reaching their target tissue they are bound to encounter and possibly interact with blood cells particularly platelets and red blood cells (RBCs). Platelets are inert carrier of oxygen which are highly sensitive than RBCs and react to external stimuli causing platelet aggregation and adhesion leading to the thrombus formation, myocardial infarction, stroke and arterial blockage. Hemocompatibility of the biomaterials is checked through the interaction of the platelets with the surface of the biomaterials [Singh et al., 2011; Singh et al., 2011, Bihari et al., 2010; Semberova et al., 2009; Jackson et al., 2011]. Recently, it has been observed that materials have the potential to induce induce integrin-mediated platelet aggregation, both in-vitro and in-vivo, on scale comparable to that obtained by thrombin which is most potent physiological agonists of platelets [Garrido et al., 2007; Rivero et al., 2012; Singh et al., 2011; Singh et al., 2011, Bihari et al., 2010]. In keeping with this observation, the hemocompatibility of the graft copolymers is checked in terms of plate function. In presence of thrombin, a known agonist, plate aggregation occurs heavily by a strong wave of cell aggregation (amplitude 80%) as observe in the tracing 4 of **Figure 3.10i**. However, pure Chitosan at lower concentration (up to 5 $\mu\text{g/ml}$ concentration) do not

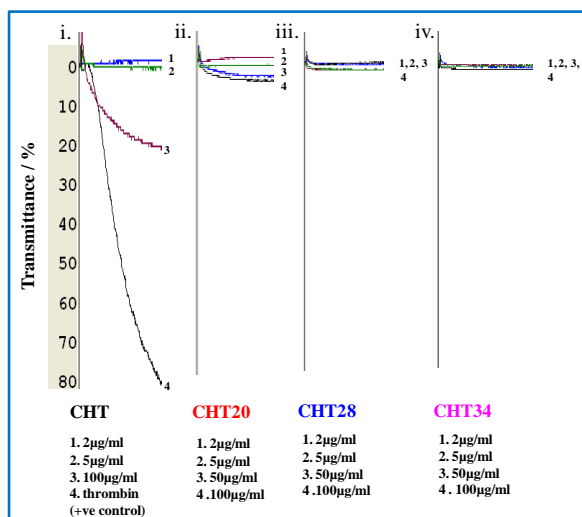


Figure 3.10: Effect of differentially modified polymers of CHT and its graft copolymer on platelet function. Platelet aggregation was induced by different concentration of reagents as indicated. Thrombin was used as a control.

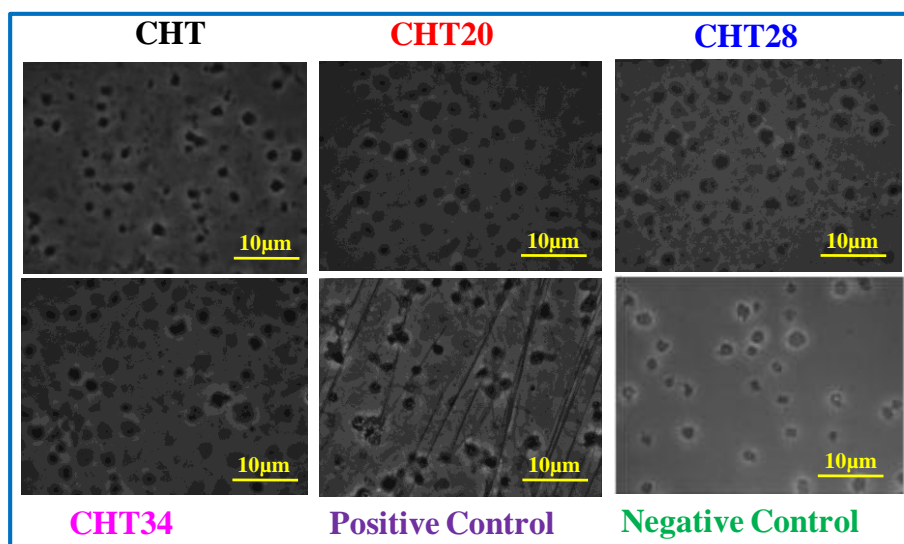


Figure 3.11: Adhesion and Spreading of platelets on immobilized matrices BSA, Collagen, on pure CHT and its indicated graft copolymers. The collagen fiber was used positive control.

exhibit platelet aggregation (tracing 1 and 2) while at higher concentration (100 µg/ml) induce significant aggregation (trace 3 of **Figure 3.10i** with the amplitude of 20%). It is nice to observed that very little aggregation (amplitude < 5%) is observed for the graft

copolymers CHT20 and CHT28 and CHT34 do not show any kind of platelet aggregation even at higher concentration of 100 $\mu\text{g/ml}$ (**Figure 3.10 iv**). Grafting of CHT with PU completely suppresses the platelet aggregation and crosslinked CHT (CHT34) is found to be best hemocompatible materials. Platelets are adhered to the exposed subendothelial surface through interaction with collagen and von Willebrand factor [Jackson et al., 2011]. Shape of the platelets is changed when the platelet surface get in touch with the tissue. In this part, adhesion of platelets with graft copolymers with different DS has shown in **Figure 3.11**. In presence of collagen matrix platelets undergo a shape change which is taken as positive control. Pure CHT and its copolymers do not exhibit any change in platelet shape, which is similar to the negative control with BSA. Hence graft copolymers are highly hemocompatible and show better result than pure polymer and maintain the platelets in resting state.

3.2.6 Erythrocyte membrane integrity and cytotoxicity of graft copolymer

Red blood cells (RBCs) are heavily found in blood. Any materials is inserted / injected into the blood stream come in contact with RBCs. Any incompatible materials disrupt the erythrocyte membrane and release their cytoplasm in the surrounding and the solution become red color. Pure CHT and its graft copolymers with same concentration are exposed to study the erythrocyte membrane integrity as shown in **Figure 3.12**. Pure CHT does not show any hemolytic activity at lower concentration (5 $\mu\text{g/ml}$) but at higher concentrations (50 and 100 $\mu\text{g/ml}$) little hemolytic activity observed. The graft copolymers (CHT20, CHT28 and CHT34) do not show any kind of hemolytic activity. Percent hemolysis of all the materials at various concentrations concentration have been reported in **Table 3.4**.

Cytotoxicity through MTT assay has been carried out to confirm the biocompatibility nature of CHT and its graft copolymers. MTT is known as the reduction of tetrazolium dye MTT to formazan in presence of viable cells by mitochondrial reductase, exhibiting purple color. Formazan production is measured after 2 hrs of exposure of materials with different concentrations (2 – 100 $\mu\text{g/ml}$) against a control of platelets without any materials. The pure CHT and its copolymers show similar viability as that of control while viability is decreased at higher concentration for CHT shown in **Figure 3.13**. It is worthy to mention that the cell viability increases with increase in DS at higher concentration and, thereby, confirm that graft copolymer is better biocompatible than

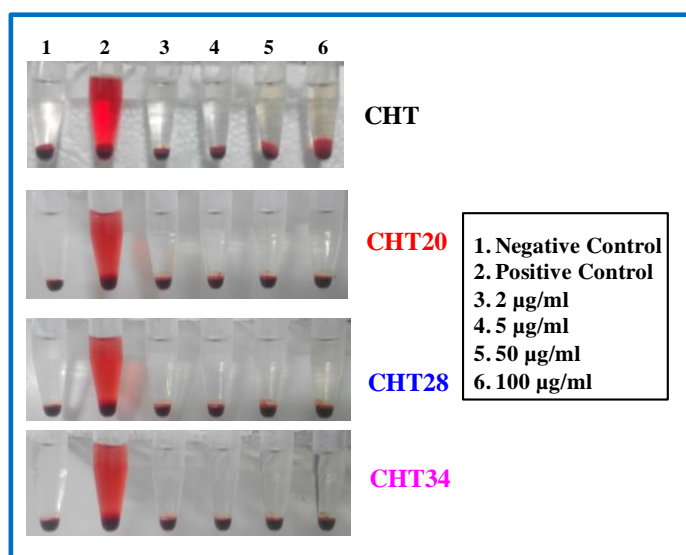


Figure 3.12: Effect of differentially functionalized polymers as indicated on erythrocyte membrane integrity. RBC suspensions were exposed to varying concentration (2, 5, 50 and 100 $\mu\text{g/mL}$) of CHT, CHT20, CHT28 and CHT34 for 4 hr followed by centrifugation. Positive and negative controls represent RBCs suspended in deionized water and RBCs suspended in phosphate buffer saline. Images of positive and negative controls are same for each experiment.

pure CHT. SDS (1 wt. %) treated platelet is taken as the positive control for MTT assay. Therefore, hemolysis study and MTT assay confirm that graft copolymers are nontoxic

and better biocompatible than pure CHT and the overall biocompatibility increases with increase in DS.

Table 3.4: Percent hemolysis of RBCs incubated with the different concentration of CHT and its Copolymers.

Concentration ($\mu\text{g / ml}$)	% of Hemolysis					Positive Control	Negative Control
	CHT	CHT20	CHT28	CHT34			
2	0	0	0	0		100	0
5	0.215	0.	0	0			
50	0.473	0.211	0.15	0			
100	0.657	0.373	0.255	0			
	CHT	CHT20	CHT28	CHT34		Positive Control	Negative Control

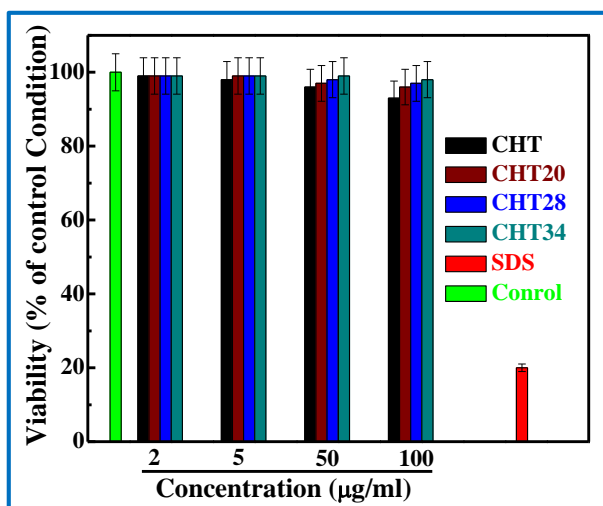


Figure 3.13: MTT assay of different copolymers-treated platelets. Mean values are reported from three independent experiments and are presented with standard deviation. SDS was used as a positive control.

Reactive oxygen species (ROS) are highly chemically reactive molecules containing oxygen which play important roles in cell signaling and homeostasis. Increment in ROS level may cause significant damage in cell structures. ROS can adversely alter protein, lipid and DNA and causes number of human diseases [Devasagayam et al., 2004; Krotz et al., 2004]. We have performed ROS generation studies to check the ability of pure CHT

and its copolymers to produce ROS. H₂DCF/DA (20 μ M)-loaded platelets are exposed to different concentrations of materials at 37 °C for 20 min, and the changes in MFI are monitored through flow cytometer (**Figure 3.14**). The result shows that at lower concentration both CHT and its graft copolymers exhibit ROS level as that of control while ROS level gradually increases with increasing concentration for pure CHT. It is interesting to know that ROS level remains low for graft copolymers even at higher concentration and ROS level gradually decreases with increasing DS of graft copolymer and exhibit lowest value in case of crosslinked copolymer (CHT34). 10 μ M H₂O₂ is used as a positive control to perform the test.

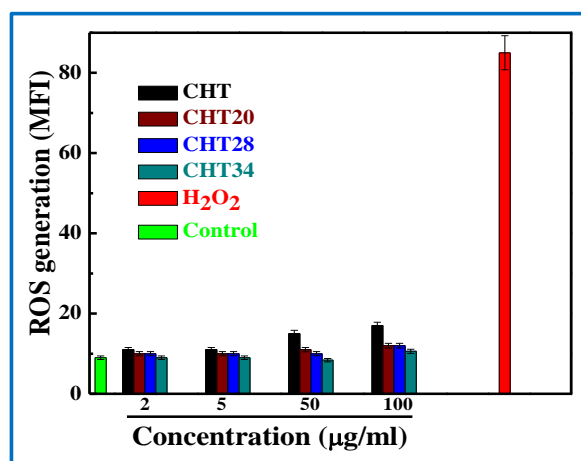


Figure 3.14: ROS generation in H₂DCF-loaded platelets treated with different concentrations of CHT, CHT20, CHT28 and CHT34 as indicated in the bar diagram.

3.2.7 Absorption of graft copolymer (CHT20) in Blood

The concentration of the materials in blood depends on the intestinal absorption of the materials [Chae et al., 2005]. Plasma concentrations of the materials are calculated on the basis of fluorescence intensity and reported in the **Figure 3.15a**. It is observed that plasma concentration of the graft copolymer (CHT20) is lower than the plasma CHT concentration. Absorption and distribution of Chitosan is mainly depends on its molecular weight (M_w) and water-solubility. Absorption and distribution of CHT

molecules increase with decrease in molecular weight and increase of the solubility [Chae et al., 2005; Zeng]. Hence, high molecular weight and low solubility of CHT20 is mainly responsible for low absorption of CHT20 than CHT. Results suggest that at 1 h absorption of the molecules is higher and decrease with time. Plasma concentration of the materials decrease as a result of distribution of the absorbed CHT20 in other organs.

3.2.8 Distribution of absorbed CHT20 in the organs

The distribution of CHT and CHT20 in organs is measured by the oral administration at predetermined time. The liver, kidney, heart, spleen, lung and thymus are investigated for the CHT and CHT20 concentration. The results show that CHT20 molecules are distributed in all the tested organs. The concentration of the materials in liver indicates the concentration of the absorption of the materials. Concentration of CHT20 in liver is gradually increased up to 4 h shown in **Figure 3.15b**. It is clear from the results that liver concentration of CHT20 is higher than the Plasma CHT20 concentration suggesting CHT20 molecules have some accumulation in liver. The distribution of the CHT20 in other tested organs has been shown in **Figure 3.15d**. The distribution of pure CHT has been shown in **Figure 3.15c**. Moreover, the histopathological examination (**Figure 3.16**) of major organs including kidney, liver and spleen shows the organs are in healthy condition similar to the control after administration of CHT20. CHT20 is distributed in all the tested organs maintaining the concentration for long period of time and do not affect the organs, so the developed system may be used as a delivery system effectively.

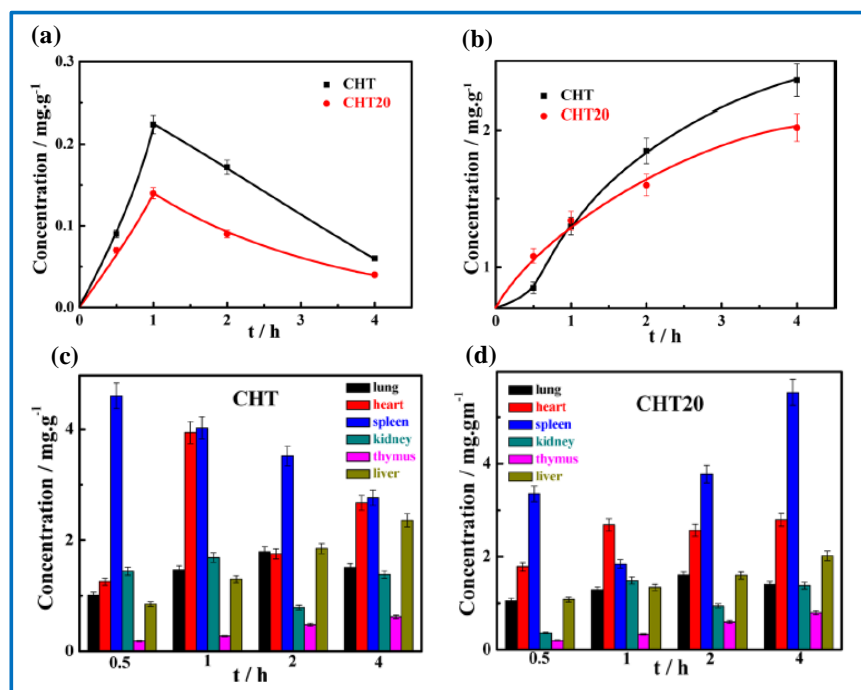


Figure 3.15: (a) plasma concentration and (b) liver concentration of CHT and CHT20 after oral administration. (C) and (d) are the concentration of CHT and CHT20 in organs.

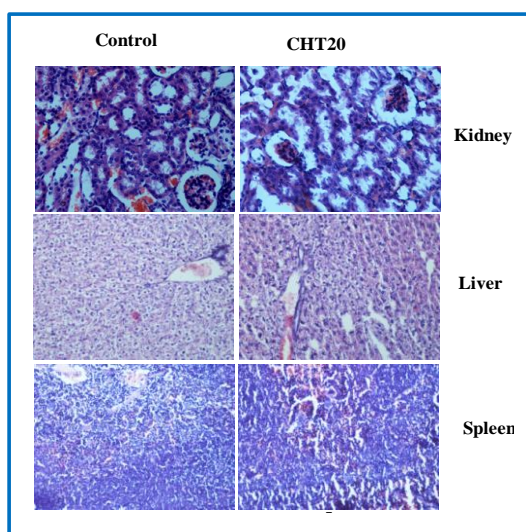


Figure 3.16: Histopathology of kidney, liver, and spleen after (a) PBS and (b) CHT20 treatment.

3.3 Conclusion

Chemical modification of chitosan has been carried out through grafting of isocyanate terminated polyurethane on to chitosan backbone and the degree of substitution has been varied until crosslinking between CHT occur molecules having polyurethane bridge. Degree of substitution has been calculated from the deconvoluted NMR peak. Spin lattice relaxation time (T_1) increases with DS due to the relaxation constraints arising from the polyurethane chain grafted on CHT molecules. Solubility and swelling properties decreases considerably with increasing DS in graft copolymers as compared to pristine CHT. Hydrophobic nature arises in Chitosan measured from the contact angle measurements which is increases with increase in degree of substitution in graft copolymers. Toughness of the copolymers is significantly increase in graft copolymers as compared to pure Chitosan while crosslinked copolymer exhibit brittle nature under uniaxial elongation. Glass transition temperature decreases in graft copolymers as observed from DMA measurement revealing flexible nature of the graft copolymers and thereby, make them suitable for applications in biomedical arena. Graft copolymers exhibit sustained release of drug suppressing the burst release observed in pure CHT. PU graft Chitosan copolymers are found to be bio- and hemocompatible in nature as observed through platelet aggregation, cell viability, cell adhesion, and hemolysis studies. Moreover, graft copolymers do not generate any reactive oxygen and the materials do not affect the biology of circulating blood cells.

Henceforth, newly developed polyurethane graft chitosan copolymers have the potential to behave as controlled drug delivery system effectively.